RadioGraphics

Cardiac PET/CT for the Evaluation of Known or Suspected Coronary Artery Disease[1]

TEACHING POINTS
See last page

Marcelo F. Di Carli, MD • Venkatesh L. Murthy, MD, PhD

Positron emission tomography (PET) is increasingly being applied in the evaluation of myocardial perfusion. Cardiac PET can be performed with an increasing variety of cyclotron- and generator-produced radiotracers. Compared with single photon emission computed tomography, PET offers lower radiation exposure, fewer artifacts, improved spatial resolution, and, most important, improved diagnostic performance. With its capacity to quantify rest–peak stress left ventricular systolic function as well as coronary flow reserve, PET is superior to other methods for the detection of multivessel coronary artery disease and, potentially, for risk stratification. Coronary artery calcium scoring may be included for further risk stratification in patients with normal perfusion imaging findings. Furthermore, PET allows quantification of absolute myocardial perfusion, which also carries substantial prognostic value. Hybrid PET–computed tomography scanners allow functional evaluation of myocardial perfusion combined with anatomic characterization of the epicardial coronary arteries, thereby offering great potential for both diagnosis and management. Additional studies to further validate the prognostic value and cost effectiveness of PET are warranted.

Abbreviations: CAC = coronary artery calcium, CAD = coronary artery disease, CFR = coronary flow reserve, ECG = electrocardiography, FWHM = full width at half maximum, LVEF = left ventricular ejection fraction, PTSM = pyruvaldehyde-bis (N4-methylthiosemicarbazone)

RadioGraphics 2011; 31:1239–1254 • **Published online** 10.1148/rg.315115056 • **Content Codes:** CA CT NM

[1]From the Division of Nuclear Medicine and Molecular Imaging, Department of Radiology, and Noninvasive Cardiovascular Imaging Program, Departments of Radiology and Medicine (Cardiology), Brigham and Women's Hospital, Harvard Medical School, 75 Francis St, ASB-L1 037-C, Boston, MA 02115 . Recipient of a Certificate of Merit award for an education exhibit at the 2010 RSNA Annual Meeting. Received March 17, 2011; revision requested April 15 and received June 22; accepted June 22. M.F.D.C. has disclosed a financial relationship (see p 1252); the other author has no financial relationships to disclose. **Address correspondence to** M.F.D.C. (e-mail: *mdicarli@partners.org*).

Funding: The work was supported in part by the National Institutes of Health [grant numbers RC1 HL101060-01 and T32 HL094301-01A1].

Introduction

Positron emission tomography (PET) has contributed immensely to the understanding of cardiac physiology and pathophysiology for more than 25 years. It is the preeminent tool for the in vivo quantification of a broad range of physiologic processes, including myocardial perfusion and metabolism, as well as neuronal and receptor function. The emerging techniques of targeted molecular imaging promise to allow the interrogation of an even broader spectrum of physiologic parameters. Although clinical use has lagged behind, it has grown steadily over the past decade, accelerating over the past 3 years. Factors contributing to this growth in clinical cardiovascular applications include *(a)* the wide dissemination of combined PET–computed tomography (CT) owing to its well-established role in the evaluation of solid and hematologic malignancies, *(b)* the regulatory approval of PET radiopharmaceuticals for cardiac imaging and subsequent reimbursement changes, *(c)* the recurrent world-wide shortages of molybdenum 99, and *(d)* increasing documentation of improved clinical effectiveness for PET/CT compared with competing modalities such as single photon emission computed tomography (SPECT). In this article, we discuss myocardial perfusion PET in terms of its technical aspects as well as its diagnostic and prognostic performance. In addition, we discuss the emerging role of cardiac PET/CT in the evaluation of patients with known or suspected coronary artery disease (CAD).

Technical Aspects of Myocardial Perfusion PET

Advantages of PET

Radiotracers used in PET undergo positive beta decay, releasing a positron, the antiparticle of an electron. The emitted positrons will travel a short distance as determined by their energy (the so-called positron range) before losing sufficient kinetic energy to interact with an electron. This interaction results in the mutual annihilation of both the positron and the electron, resulting in the emission of two photons of equal energy (511 keV) and opposite direction. PET relies on the nearly simultaneous detection of these two photons on opposite sides of a circular array of detectors. By relying on two coincident photons per decay, PET systems provide increased spatial resolution and decreased noise compared with single-photon methods such as SPECT. The axial spatial resolution of modern PET scanners ranges from 5 to 6.3 mm full width at half maximum (FWHM), depending on scanner configuration and location in the field of view. This is poorer than the spatial resolution of magnetic resonance (MR) imaging and CT and allows reporting of only the transmural distribution of myocardial perfusion.

Imaging Agents for Clinical Use

Table 1 describes radiopharmaceuticals that have been used for the PET evaluation of myocardial perfusion in humans. ^{82}Rb is a potassium analog with kinetic properties similar to those of thallium 201 (^{201}Tl) (1). Because it is a generator product, ^{82}Rb is the most widely used radionuclide for the assessment of myocardial perfusion with PET. Its parent radionuclide is ^{82}Sr, which has a physical half-life of 26 days. Consequently, the ^{82}Sr/^{82}Rb generator is replaced every 4 weeks. The short physical half-life of ^{82}Rb and the rapid reconstitution of the generator allow fast sequential perfusion imaging and laboratory throughput, thereby maximizing clinical efficiency.

The maximum kinetic energy of positrons emitted during ^{82}Rb decay is significantly higher than that for ^{18}F or ^{13}N. Consequently, the spatial uncertainty in the location of the decaying nucleus—which depends on the distance traveled by the positrons before they are annihilated (positron range)—is greater for ^{82}Rb (2.6 mm FWHM) than for ^{18}F (0.2 mm FWHM) or ^{13}N (0.7 mm FWHM). This results in decreased spatial resolution for ^{82}Rb compared with these other radiotracers. Although ^{82}Rb imaging yields excellent image quality with current PET technology, the combination of a greater positron range and a short half-life, which necessitates significant image smoothing to suppress noise, partially negates the improved spatial resolution of PET.

^{13}N-ammonia requires an onsite cyclotron and radiochemical synthesis capability. The first-pass myocardial extraction of ^{13}N-ammonia at rest (ie, the fraction of activity transported from the vascular space into the myocardium at first-pass perfusion) is extensive, although as with other extractable radiotracers (eg, ^{82}Rb), it decreases at higher blood flow rates. If first-pass extraction is extensive, radiotracer accumulation in the myocardium

Table 1
Radiopharmaceuticals Used for Myocardial Perfusion PET

Radiotracer	Physical Half-Life	Availability	FDA Status	Advantages	Disadvantages
Rubidium 82 (^{82}Rb)	76 sec	Strontium 82 (^{82}Sr)/^{82}Rb generator	Approved	Simplicity of use	Relatively poor resolution
Nitrogen 13 (^{13}N)–ammonia	10 min	Cyclotron	Approved	High extraction simplifies quantitation	Requires cyclotron, heterogeneous uptake
Copper 62 (^{62}Cu)–pyruvaldehyde-bis (N4-methylthiosemicarbazone) (PTSM)	10 min	^{62}Zn/^{62}Cu generator	Not approved*	Rapid blood pool clearance, long myocardial retention	Short parent isotope half-life
Oxygen 15 (^{15}O)–water	2 min	Cyclotron	Not approved	Diffusible with high extraction under a variety of conditions	Requires cyclotron, images not suitable for clinical imaging
Fluorine 18 (^{18}F)–flurpiridaz	110 min	Cyclotron	Not approved†	Long half-life allows unit dose distribution and exercise studies	Not FDA approved, higher radiation dose for same-day stress-rest studies due to long half-life

Note.—FDA = U.S. Food and Drug Administration.
* ^{62}Cu-PTSM is currently under investigation for clinical use.
† ^{18}F-flurpiridaz is currently entering Phase III investigation for clinical use.

will be proportional to myocardial blood flow, simplifying quantitation of myocardial perfusion. Unfortunately, regional myocardial retention of ^{13}N-ammonia may be heterogeneous: The lateral wall of the left ventricle tends to have lower activity than do other segments. ^{13}N-ammonia images may also occasionally be degraded by intense activity in the lung (especially in patients with heart failure) or liver, which can interfere with evaluation of the inferior and lateral walls, respectively.

^{62}Cu-PTSM is produced from the elution of zinc 62 (^{62}Zn) generators. The degree of single-pass extraction of ^{62}Cu-PTSM is similar to that of ^{13}N-ammonia, with a markedly prolonged myocardial retention and rapid blood pool clearance (2–4). In animal studies, the myocardial activity appears to correlate with microsphere-determined blood flow, although as with other extractable radiotracers there is a plateau in net extraction at relatively high flows (5,6). One disadvantage of the use of ^{62}Cu-PTSM is the relatively short half-life of the parent radioisotope (^{62}Zn [half-life = 9.1 hours]), which necessitates daily delivery of ^{62}Zn/^{62}Cu generators, thereby limiting practical application. Nonetheless, use of this agent is still under investigation (7).

^{15}O-water is a cyclotron product with a physical half-life of approximately 2 minutes. It is a freely diffusible agent with extensive myocardial extraction across a wide range of myocardial blood flows (1). The degree of extraction is independent of flow and is not affected by the metabolic state of the myocardium (1). However, because ^{15}O-water is a freely diffusible agent, imaging is challenging due to its high concentration in the blood pool, requiring additional postprocessing for visualization of the myocardium. Its use is limited to research applications.

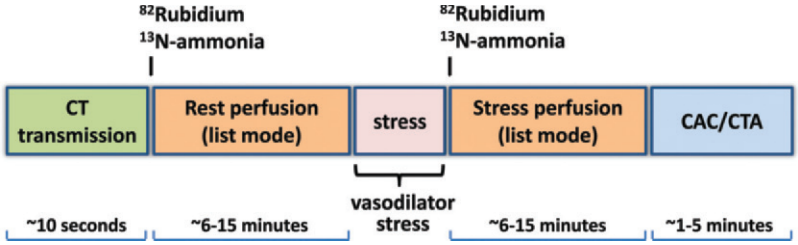

Figure 1. State-of-the-art hybrid cardiac PET/CT protocol for delineation of the extent and functional consequences of atherosclerosis. With use of an integrated PET/CT imaging system, both anatomic CAD and resulting myocardial ischemia can be characterized in a single setting. In patients with known CAD, the coronary artery calcium (CAC) scan may be omitted (although its use may be helpful for identifying patients who have extensive coronary calcification and are thus poor candidates for nonenhanced CT angiography *[CTA]* performed with a relatively low radiation dose). Alternatively, if detailed delineation of the extent of CAD is not required, the CAC scan alone, without coronary CT angiography, may allow additional risk stratification at lower radiation doses without iodinated contrast material. Because the attenuation-correction CT is not electrocardiographically (ECG) gated and is performed during free breathing to best match the PET study, it is not useful for quantitative ascertainment of the calcium score. However, approximate evaluation of the calcium score from attenuation-correction CT images may be possible (15).

^{18}F-flurpiridaz is a pyridaben derivative that binds to the mitochondrial complex 1 (MC-1) inhibitor (8–10). Animal and human studies demonstrate homogeneous myocardial uptake with very good activity ratios between myocardium and blood, liver, and lung. ^{18}F-flurpiridaz shows extensive first-pass extraction across a wide range of myocardial blood flows (8–11). Phase I and phase II clinical studies have been completed, and the U.S. Food and Drug Administration has recently approved plans for phase III development (12). One potential advantage of the use of this agent is that the ^{18}F radiolabel (as with 2-[fluorine-18]fluoro-2-deoxy-D-glucose) will allow unit dose distributions, which will facilitate broader access to cardiac PET. Furthermore, the long half-life of the ^{18}F label (109.8 minutes) will permit routine exercise stress testing.

Advances in PET Technology

Several key developments in hardware and software have contributed to improved technical performance of modern PET systems. New detector technology has improved overall count detection sensitivity and spatial resolution (13). Increased detector sensitivity combined with optimization of scanner electronics and improved image reconstruction algorithms have substantially improved overall image quality and permit decreased patient doses compared with prior-generation PET systems (14). The optimization of list-mode imaging has been particularly important for cardiac imaging because it allows multiple image reconstructions (see the following section) from a single acquisition, thereby facilitating a more comprehensive examination (Fig 1). In list mode, spatial data for every coincident pair of photons are recorded sequentially with very high temporal resolution along with the associated electrocardiographic phase, providing maximal flexibility for the offline reconstruction of summed, gated, or dynamic images during postprocessing at the expense of increased data storage requirements.

Dedicated software for routine correction of misalignments between transmission and emission images has helped reduce the frequency of artifacts and improve diagnostic accuracy. The emergence of integrated PET/CT technology as the dominant configuration of clinical scanners holds great promise for cardiac imaging, since it permits combined examinations that can delineate both the anatomic extent of epicardial coronary atherosclerosis and the physiologic consequence of these lesions (ie, impaired myocardial perfusion). Integrated PET/MR imagers are currently in development and will expand the possibilities for the combined characterization of myocardial tissue architecture and physiology (16).

Table 2
Average Effective Radiation Doses for Myocardial Perfusion PET and SPECT

Protocol	Average Effective Dose from MPI (mSv)*	Average Effective Dose from CT Attenuation Correction (mSv)†	Average Total Effective Dose (mSv)
One-day technetium 99m (^{99m}Tc) SPECT	9.9–11.4	0.5	10.9–12.4
Two-day ^{99m}Tc SPECT	12.8–15.7	0.5	13.8–16.7
^{201}Tl/^{99m}Tc SPECT	29.3	0.5	30.3
Stress-only ^{99m}Tc SPECT	7.1–8.0	0.5	8.1–9.0
^{13}N-ammonia PET	2.2	0.5	2.7
^{82}Rb PET	3.7	0.5	4.2

Note.—MPI = myocardial perfusion imaging.
*Estimated using injected doses per American Society of Nuclear Cardiology guidelines (21). ^{82}Rb dosimetry estimated according to references 18 and 22.
†CT attenuation dose is based on typical protocols used for cardiac imaging. Attenuation correlation for SPECT assumes two separate scans (stress and rest).

Optimized Protocols for Myocardial Perfusion Imaging

Figure 1 illustrates a state-of-the-art imaging protocol. The use of list-mode imaging allows multiple image reconstructions from a single imaging dataset (ie, summed, ECG gated, and multiframe or dynamic) for a comprehensive physiologic examination of the heart. With this approach, image acquisition starts with the bolus injection of the radiopharmaceutical and continues for 6–7 minutes after ^{82}Rb injection and for approximately 10–20 minutes after ^{13}N-ammonia injection. Stress testing is most commonly performed with pharmacologic agents (eg, vasodilators or dobutamine), but testing during exercise is also possible (17). The latter testing is more straightforward with ^{13}N-ammonia (half-life ≅ 10 minutes) than with ^{82}Rb (half-life = 76 seconds).

After completion of stress-rest PET, patients who are not known to have CAD will generally undergo low-dose scanning to ascertain the presence of coronary artery calcifications. This study may be omitted in patients with known CAD; however, because patients with extensive calcifications may not be good candidates for CT angiography, this study can help avoid unnecessary exposure to contrast material and radiation in patients in whom diagnostic-quality images are unlikely to be obtained. Patients undergoing coronary CT angiography are generally treated with sublingual nitroglycerin to maximize coronary vasodilation and with β-adrenergic blocking agents to slow the heart rate to approximately 60 bpm or lower to maximize CT angiographic image quality. Prospective ECG triggering or ECG-triggered tube current modulation results in lower radiation exposures but requires slow, regular heart rates.

Radiation Dosimetry

PET with the use of short-lived radiopharmaceuticals results in substantially lower radiation doses to patients than does SPECT (18). Recent data suggest that the total-body effective dose from a stress-rest myocardial perfusion study performed with ^{82}Rb is approximately 4 mSv (19,20). The total-body effective dose from a stress-rest myocardial perfusion study performed with ^{13}N-ammonia and ^{15}O-water is less than 3 mSv (Table 2) (18).

Teaching Point

Recognizing and Preventing Imaging Artifacts at Cardiac PET/CT

Although severe artifacts resulting in suboptimal imaging are far less common with PET than with SPECT (23), artifacts due to errors in attenuation correction are common and have been reported with PET/CT in 30%–60% of cases (24,25). These artifacts are usually related to misalignments between the CT transmission and emission datasets caused by patient, cardiac, or respiratory motion (25,26), and may lead to false regional defects in some cases (Fig 2) (27). Patient motion at SPECT may be detected with inspection of rotating projection images; however, due to the circular array of scintillation detectors in PET/CT

Teaching Point

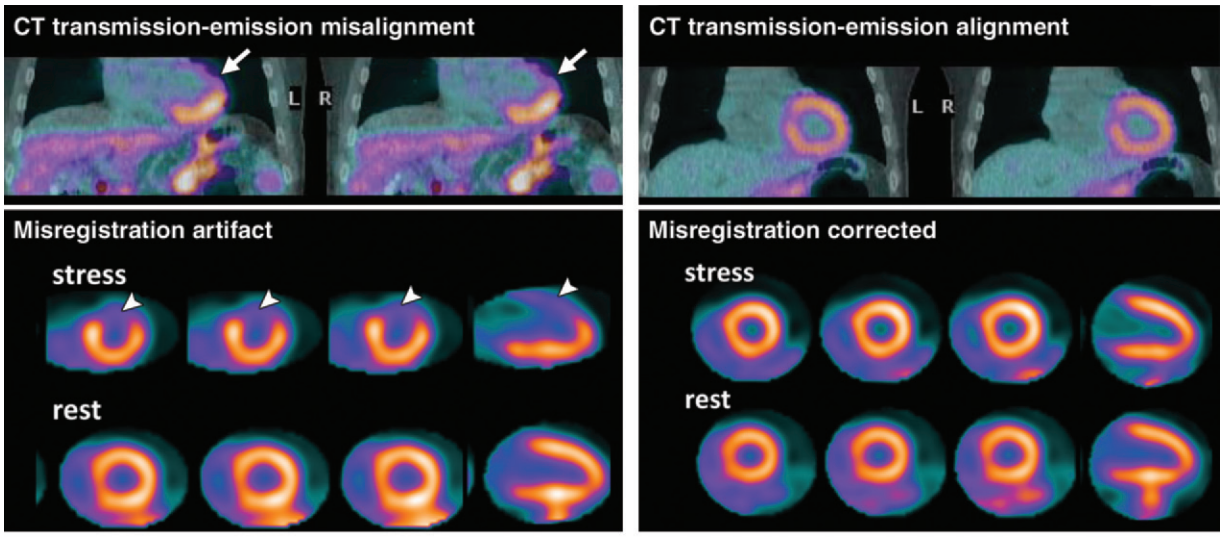

Figure 2. PET artifact caused by transmission-emission misalignment. **(a)** Misalignment of CT transmission and emission (^{82}Rb) images (top) is a result of the anterior and anterolateral walls overlapping the lung field (arrow). Consequently, the stress-rest myocardial perfusion PET scans (bottom) show an apparent reversible anterior and anterolateral perfusion defect (arrowhead). This typical perfusion defect results from applying low-attenuation coefficients (corresponding to air) to the myocardial region overlapping the lung field on the CT transmission scan during tomographic reconstruction. **(b)** Correctly aligned transmission-emission images (top) result in a normal perfusion study (bottom).

Table 3
Summary of Published Studies Documenting the Accuracy of Myocardial Perfusion PET in Detecting Obstructive CAD

Author	Total No. of Patients	Women Patients (%)	Patients with Prior CAD (%)	PET Radiotracer	Sensitivity (%)	Specificity (%)	PPV (%)	NPV (%)	Accuracy (%)
Sampson et al (28)	102	42	0	^{82}Rb	93	83	80	94	87
Bateman et al (29)	112	46	25	^{82}Rb	87	93	95	81	89
Marwick et al (30)	74	19	49	^{82}Rb	90	100	100	36	91
Grover-McKay et al (31)	31	1	13	^{82}Rb	100	73	80	100	87
Stewart et al (32)	81	36	42	^{82}Rb	83	86	94	64	84
Go et al (33)	202	NR	47	^{82}Rb	93	78	93	80	90
Demer et al (34)	193	26	34	^{82}Rb/^{13}N-ammonia	83	95	98	60	85
Tamaki et al (35)	51	NR	75	^{13}N-ammonia	98	1	100	75	98
Gould et al (36)	31	NR	NR	^{82}Rb/^{13}N-ammonia	95	1	100	90	97
Weighted summary	877	29	35		90	89	94	73	90

Source.—Reference 37.
Note.—NPV = negative predictive value, NR = not reported, PPV = positive predictive value.

cameras, patient movement during PET affects all projections and can be very difficult to detect. Because transmission imaging and emission imaging are sequential, patient or respiratory (eg, from deep inspiration) motion during emission imaging will most likely lead to transmission-emission misalignment and potential attenuation-correction artifacts (Fig 2). The extent and direction of this

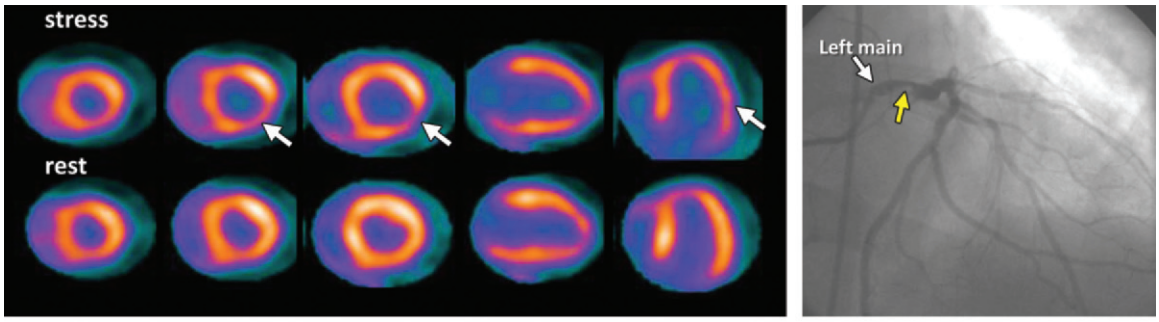

a. b.

Figure 3. Underestimation of CAD extent at PET in a 63-year-old man who was referred for evaluation of atypical chest pain. **(a)** Stress-rest myocardial perfusion PET scans demonstrate a small reversible perfusion defect involving the inferolateral wall (arrow), a finding that is consistent with single-vessel ischemia in the left circumflex–obtuse marginal coronary artery territory. Although PET helped correctly identify the patient as having obstructive CAD, it led to severe underestimation of the amount of myocardium at risk. **(b)** Left anterior oblique coronary angiogram reveals severe stenosis (yellow arrow) of the left main artery (white arrow).

misalignment will determine whether artifacts will be apparent on the attenuation-corrected images. Proper quality control and availability of registration software are crucial prior to interpretation of SPECT/CT and PET/CT images.

Diagnostic and Prognostic Performance of Myocardial Perfusion PET

Table 3 summarizes the published studies documenting the diagnostic accuracy of myocardial perfusion PET for detecting obstructive CAD. The average weighted sensitivity for detecting at least one coronary artery with more than 50% stenosis is 90% (range, 83%–100%), whereas the average specificity is 89% (range, 73%–100%). The corresponding average positive and negative predictive values are 94% (range, 80%–100%) and 73% (range, 36%–100%), respectively, and the overall diagnostic accuracy is 90% (range, 84%–98%).

Comparison with SPECT

Three studies have compared the diagnostic accuracy of ^{82}Rb myocardial perfusion PET and ^{201}Tl or ^{99m}Tc SPECT in the same (32,33) or matched (29) patient populations. A recent study by Bateman et al (29) is particularly important because it compared ^{82}Rb PET and ^{99m}Tc sestamibi SPECT in two matched patient cohorts undergoing clinically indicated pharmacologic-stress perfusion imaging using contemporary technology for both SPECT and PET. Overall diagnostic accuracy with a stenosis threshold at angiography of either 50% or 70% was higher for PET than for SPECT (87% versus 71% and 89% versus 79%, respectively) (29). Improved accuracy was driven primarily by the increased specificity of PET compared with SPECT, along with a marginal advantage in sensitivity. This improved diagnostic accuracy persisted in several key subgroups, which included both men and women as well as both obese and nonobese individuals. The high prevalence of significant attenuation artifacts at SPECT among obese persons highlights the value of PET in these individuals.

Detection of Multivessel CAD

Teaching Point

Although the assessment of myocardial perfusion with PET remains a sensitive means of diagnosing or ruling out the presence of obstructive CAD in individual patients, PET (like SPECT) often helps identify only the coronary territory affected by the most severe stenoses. This is because coronary vasodilator reserve is globally reduced in patients with diffuse CAD, leading to so-called balanced reduction in myocardial perfusion and limiting detection of multivessel coronary artery stenosis (Fig 3). Other manifestations of balanced ischemia may include transient ischemic dilatation of the left ventricular cavity and the absence of stress-induced left ventricular ejection fraction (LVEF) augmentation, although these are likely less sensitive signs than is impaired coronary vasodilator reserve (described later).

Quantification of Left Ventricular Function

A distinct advantage of ECG-gated PET is its capacity to assess left ventricular function at rest and during peak stress (as opposed to poststress assessment with gated SPECT). Recent data from our laboratory suggest that in healthy subjects, LVEF increases during peak vasodilator stress (38). However, this increase in LVEF (from baseline to peak stress) is inversely related to the magnitude

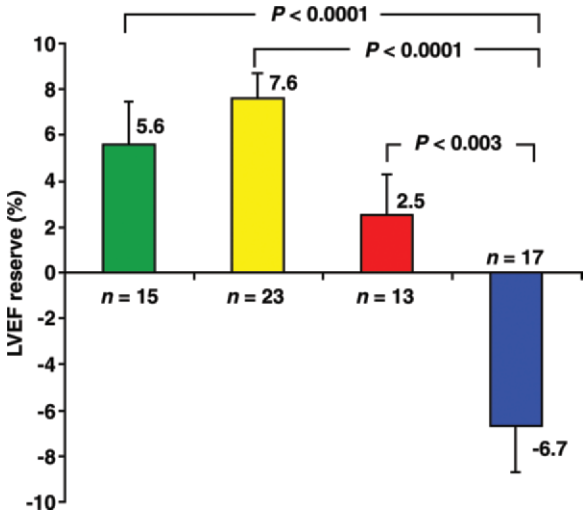

Figure 4. Relationship between the extent of CAD and LVEF reserve. Bar graph demonstrates the inverse relationship between the extent of angiographic CAD (>70% stenosis) and the stress-induced change in LVEF. Each bar represents the mean LVEF reserve (ie, change in LVEF from rest to peak stress) on gated perfusion PET scans obtained in patients with 0- (green), 1- (yellow), 2- (red), or 3-vessel or left main (blue) CAD at invasive coronary angiography. (Reprinted, with permission, from reference 38.)

Figure 5. Use of CFR to identify disease not visible at perfusion PET in a 61-year-old man who was referred for evaluation of chest pain. **(a, b)** Stress-rest myocardial perfusion PET scans **(a)** demonstrate a small reversible perfusion defect involving the left ventricular apex and inferoapical segments, a finding that is consistent with single-vessel ischemia in the distal left anterior descending coronary artery territory. Although PET helped correctly identify the patient as having obstructive CAD, it led to severe underestimation of the amount of myocardium at risk. However, quantitative CFR **(b)** was markedly impaired in all vascular territories (normal CFR >2), a finding that is consistent with extensive ischemic myocardium. *LAD* = left anterior descending artery, *LCX* = left circumflex artery, *RCA* = right coronary artery. **(c, d)** Left anterior oblique coronary angiograms (**d**, caudal view) demonstrate a complex plaque causing 70% stenosis involving the distal left main, proximal LAD, and LCX arteries (arrowheads). The right coronary artery had nonobstructive atherosclerosis.

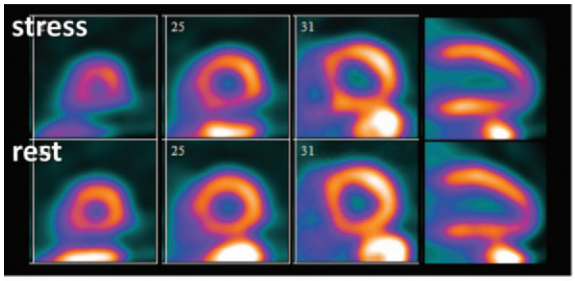

a.

	LAD	LCX	RCA	Global
CFR	1.14	1.07	1.28	1.17

b.

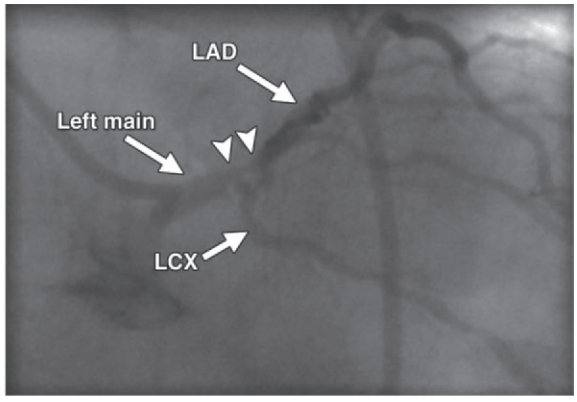

c.

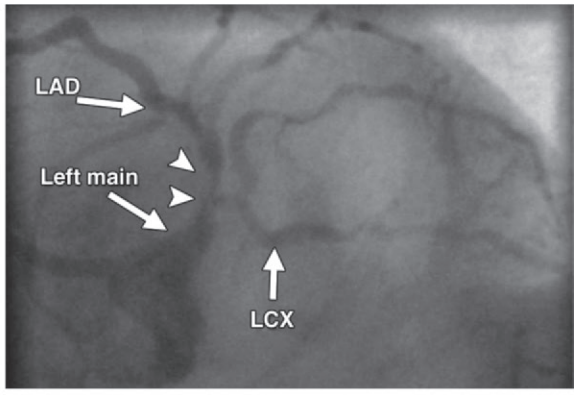

d.

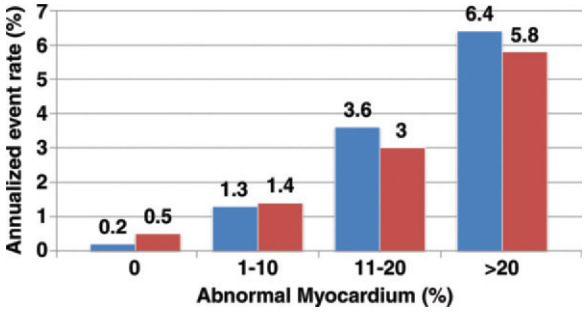

Figure 6. Relationship between predicted mortality and stress perfusion defects. Bar graph demonstrates the increased unadjusted annualized rate of cardiac death (blue) and myocardial infarction (red) with increasing extent and severity of perfusion defects at stress PET in patients with known or suspected CAD. (Adapted, with permission, from reference 41.)

of ischemia and the extent of angiographic CAD (38,39). In patients with multivessel CAD, LVEF often shows a blunted response or a frank drop during peak stress (Fig 4). The negative predictive value of a stress-induced increase in LVEF of 5% or more for excluding the presence of multivessel CAD is high (>90%). This change in LVEF during peak stress has also been shown to have value for risk prediction (40,41).

Quantification of Myocardial Blood Flow and Flow Reserve

PET measurements of myocardial blood flow (in milliliters per minute per gram of myocardium) and coronary flow reserve (CFR) (the ratio between myocardial blood flow at peak stress and myocardial blood flow at rest) can also be used to establish the presence of multivessel CAD. Indeed, there is consistent evidence that estimates of coronary vasodilator reserve made with PET are inversely and nonlinearly related to the severity of stenosis (42–44). Although these relationships were originally established with the use of ^{13}N-ammonia and ^{15}O-water as flow tracers, similar quantitative information can be obtained with ^{82}Rb (45–47). This stepwise reduction in myocardial perfusion reserve can be used to detect flow-limiting disease in myocardial regions, showing relatively normal radiotracer uptake due to balanced flow reduction (Fig 5). Proof-of-concept studies in up to 27 patients have shown that these quantitative estimates of CFR with PET allow better definition of the extent of anatomic CAD (48,49). However, it is important to note that myocardial perfusion quantitation with PET methods cannot help differentiate decreased perfusion due to epicardial coronary artery stenosis from that due to microvascular dysfunction. Hybrid PET–coronary CT angiography may be particularly helpful in this regard.

Risk Prediction

With the increased clinical use of PET and PET/CT in stress myocardial perfusion imaging, observational data documenting its incremental prognostic value are beginning to emerge. The prognostic value of dipyridamole stress ^{82}Rb PET was recently investigated in 367 patients, who were followed up for 3.1 ± 0.9 years (23). As has been previously described with SPECT, the increasing extent and severity of perfusion defects with stress PET were associated with increased frequency of adverse events. According to a study by Yoshinaga et al (23), the rate of occurrence of "hard events" (ie, myocardial infarction or cardiac death) in patients with normal stress PET findings was 0.4% per year. However, this study was limited by the occurrence of only 17 hard events. More recent data from our laboratory in a larger patient cohort (n = 1432, with 113 deaths) demonstrated that increases in the extent and severity of stress perfusion defects translated into proportional increases in predicted mortality, even after adjusting for other important prognostic markers (Fig 6) (41). These data also confirmed that LVEF and stress perfusion imaging yield independent and additive prognostic information. This analysis showed that the mortality hazard was inversely related to LVEF. Furthermore, myocardial perfusion imaging added incremental value to LVEF (at any LVEF, a higher summed stress score indicated greater risk), and LVEF added incremental value to myocardial perfusion imaging (ie, at any summed stress score, a lower LVEF indicated greater risk) (41).

Teaching Point

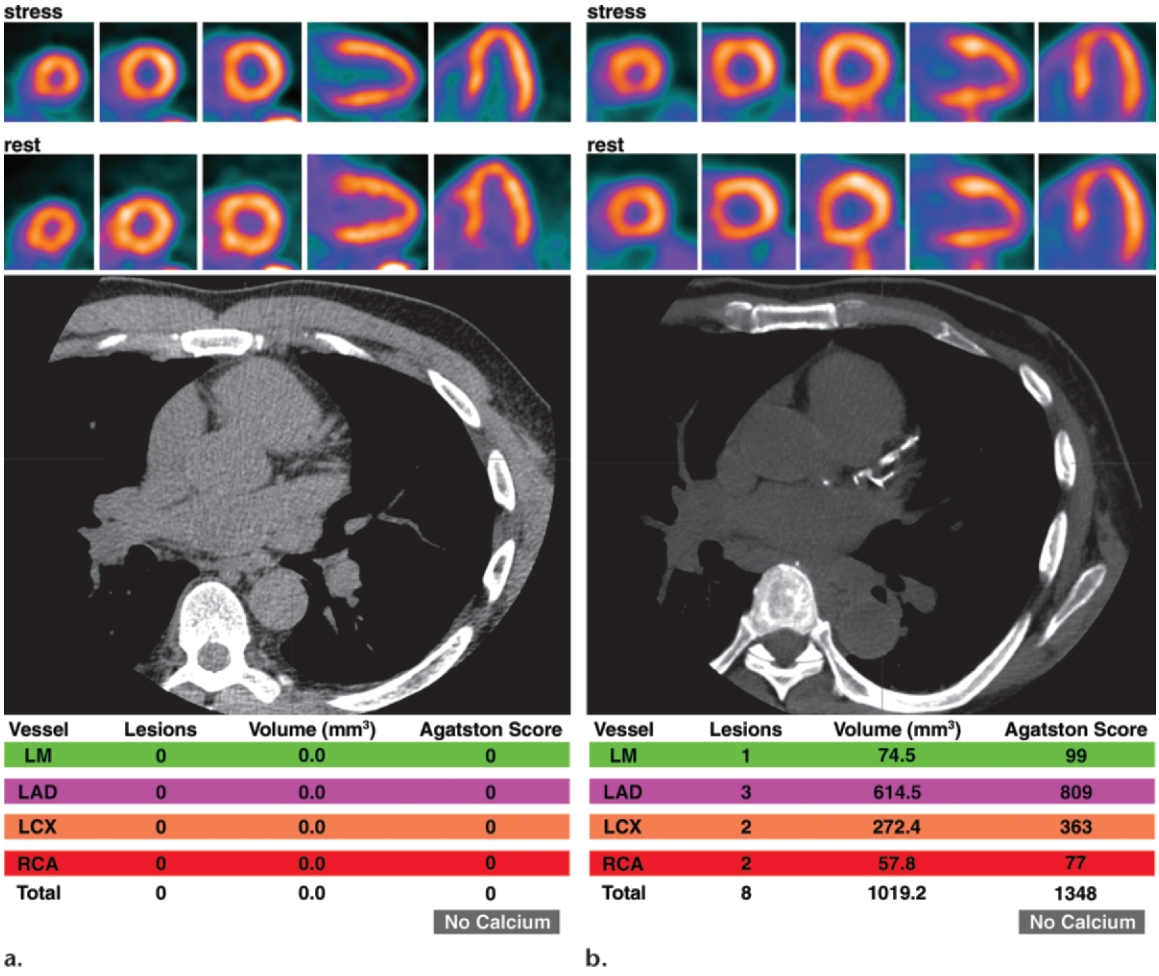

Figure 7. Potential added value of a CAC score in patients with normal myocardial perfusion who had been referred for evaluation of atypical angina. **(a)** Stress-rest myocardial perfusion PET images (top) and a representative transverse section from a nonenhanced gated cardiac CT scan (middle) obtained in a 61-year-old man with dyslipidemia and hypertension demonstrate no evidence of coronary artery calcifications (Agatston score = 0 [bottom]). **(b)** Stress-rest myocardial perfusion PET images (top) and a representative transverse section from a nonenhanced gated cardiac CT scan (middle) obtained in a 59-year-old man with dyslipidemia and a family history of CAD demonstrate coronary artery calcifications that are, however, not extensive (Agatston score = 1348 [bottom]). In both **a** and **b**, the normal myocardial perfusion PET scans indicate no evidence of flow-limiting CAD, suggesting an equally low risk in both patients. However, the CAC scores indicate very different degrees of atherosclerosis, suggesting a higher risk in the patient with extensive coronary calcifications. *LAD* = left anterior descending artery, *LCX* = left circumflex artery, *LM* = left main coronary artery, *RCA* = right coronary artery.

Improvement of Risk Stratification with CFR Estimates

Teaching Point

The difficulties in identifying balanced flow reduction in high-risk patient groups (eg, patients with diabetes mellitus or renal dysfunction) can be overcome with quantitative myocardial perfusion measures. Thus, better delineation of at-risk myocardium with quantitative CFR may also improve risk stratification in patients with known or suspected CAD. A study of 289 asymptomatic patients at low to intermediate risk but without overt CAD demonstrated a stepwise reduction in CFR, with the estimated 10-year risk of congenital heart disease obtained on the basis of a Framingham score (50). Although this study did not examine the prognostic value of CFR, the findings provided initial evidence that such quantitative measures of jeopardized myocardium could improve risk stratification in patients with known or suspected CAD. A relatively small recent study of 256 patients with known or suspected CAD demonstrated incremental risk stratification with CFR compared with clinical variables and semi-

quantitative measures of myocardial perfusion (51). Unfortunately, this study included relatively few hard events (29 cardiac deaths) and was underpowered to fully explore the relationship between CFR estimates and prognosis. In addition, multivariable modeling was incomplete, since key predictors of prognosis (eg, LVEF) were not included or explored. Nonetheless, the data suggest that quantitative imaging may be valuable for refining our traditional estimates of clinical risk.

Emerging Clinical Role of Integrated PET/CT

Integrated PET–multidetector CT has interesting potential for cardiac imaging. This technology allows detection and quantification of the burden of calcified and noncalcified plaques, quantification of vascular reactivity and endothelial health, identification of flow-limiting coronary stenoses, and, potentially, identification of high-risk plaques (through fusion of anatomic and biologic information obtained with targeted molecular imaging) in the coronary and other arterial beds (eg, cerebral, mesenteric, renal) in the same setting.

Potential Added Value of CAC Score in Patients with Normal Myocardial Perfusion

The potential to measure stress-rest myocardial perfusion and obtain a nonenhanced CT CAC score with a single dual-modality study may offer a unique opportunity to expand the prognostic value of stress nuclear imaging. The rationale for this integrated approach is predicated on the fact that the perfusion imaging approach is designed to uncover only obstructive stenosis and, thus, is insensitive for detecting subclinical atherosclerosis (Fig 7). The CAC score reflects the anatomic burden of atherosclerosis but does not help localize disease or identify functional ischemia. Recent evidence comparing the results of cardiac CT and myocardial perfusion imaging suggests that a significant proportion of patients with suspected CAD but normal myocardial perfusion (reflecting the absence of flow-limiting disease) have evidence of subclinical (and sometimes extensive) atherosclerosis at CAC scoring (52–54). Integrated assessment of functional ischemia with myocardial perfusion imaging and quantification of the overall atherosclerosis burden with CAC scoring may improve risk assessment and allow more rational and cost-effective individualization of the intensity and goals of medical therapy. For example, two recent studies have shown that in patients with normal myocardial perfusion, there is a stepwise increase in the risk of adverse events (death and myocardial infarction) with increasing CAC scores. The annualized event rate for patients with a CAC score of 0 ranged from 0.7% to 2.4%, whereas for patients with a CAC score of 400 or more, it ranged from 3% to 11% (53,54). The relatively wide range in the annualized event rates likely reflects the different underlying clinical risks for patients in the two studies, one of which included mostly asymptomatic patients (54), whereas the other evaluated symptomatic patients (53). Although it is premature to predict the clinical significance of these observations, they do provide an intriguing basis for future investigations of the potential complementary role of CT and perfusion imaging for individualizing risk stratification and case management. Although myocardial perfusion imaging will likely continue to define the need for revascularization, the objective assessment of atherosclerotic burden with CAC scoring may play a role in individualizing the intensity and goals of therapy.

Potential Added Value of Coronary CT Angiography in Patients with Equivocal Myocardial Perfusion PET Findings

The incorporation of quantitative CFR information in the clinical interpretation of myocardial perfusion PET scans presents potential challenges. As discussed earlier, quantitative flow reserve data increase the sensitivity of PET for detecting flow-limiting stenosis, especially in the setting of multivessel CAD (48,49). However, there is an extensive literature demonstrating that quantitative myocardial blood flow and flow reserve estimates are affected by coronary risk factors associated with endothelial dysfunction and microvascular disease, even in the absence of overt cardiovascular disease (55–59). Consequently, the link between impaired flow reserve and obstructive epicardial disease is confounded by the association between impaired vascular reactivity and coronary risk factors that are highly prevalent in patients undergoing testing for suspected CAD. Recent data obtained in patients undergoing hybrid PET–CT angiography who were subsequently referred for invasive coronary angiography and functional evaluation on the basis of fractional flow reserve illustrate this point (60). By helping identify epicardial stenosis, CT angiography increased the specificity and positive predictive value of the quantitative flow reserve

Table 4
Diagnostic Performance of Hybrid PET/CT

Modality	Sensitivity (%)	Specificity (%)	PPV (%)	NPV (%)	Accuracy (%)
CTA	95	87	81	97	90
PET	95	91	86	97	92
PET + CTA	95	100	100	98	98

Source.—Reference 60.
Note.—CTA = CT angiography, NPV = negative predictive value, PPV = positive predictive value.

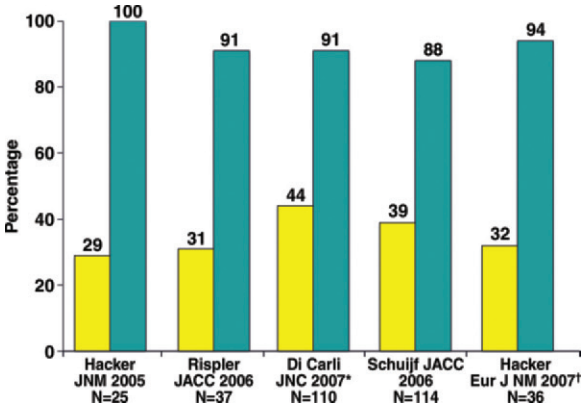

Figure 9. Positive predictive value of CT angiography for identifying flow-limiting coronary stenoses. Bar graph illustrates the frequency with which inducible ischemia occurs at myocardial perfusion imaging in territories with over 50% stenosis at coronary CT angiography. Yellow = positive predictive value, blue = negative predictive value, * = Di Carli study used PET, † = Hacker study used 64-section multidetector CT. (Reprinted, with permission, from reference 37.)

measures made with PET for the identification of flow-limiting disease (Table 4). Such strategies help distinguish patients with epicardial stenosis, in whom referral for subsequent cardiac catheterization and revascularization can be of potential clinical benefit, from those with impaired microvascular function, in whom optimization of medical therapy is preferable to invasive management.

Potential Added Value of Myocardial Perfusion PET in Patients with Apparent CAD at Coronary CT Angiography

Because not all coronary stenoses detected with CT angiography are flow limiting, the stress myocardial perfusion PET data complement the CT anatomic information by providing instant assessment of the functional significance (ie, ischemic burden) of such stenoses (Fig 8). Recent data from multiple laboratories using either sequential imaging (CT angiography followed by SPECT) or hybrid imaging (SPECT/CT or PET/CT) suggest that the positive predictive value of CT angiography for identifying flow-limiting coronary stenoses is suboptimal (Fig 9) (61–65). These findings are consistent with the well-described limitations of anatomic measures of CAD for the delineation of physiologically meaningful stenoses (66), a problem compounded by the inherent imprecision of CT compared with conventional coronary angiography due to its lower temporal and spatial resolution and its increased susceptibility to calcium-related artifacts (60,67). Stress perfusion imaging is important in this clinical scenario for confirming the functional significance of a lesion and for delineating the magnitude of ischemic myocardium so as to identify patients who may benefit from revascularization, while at the same time avoiding unnecessary catheterizations, which expose patients to risk and entail additional costs (68). This is supported by a growing body of evidence from large observational and randomized clinical trial data (69–72). Together, these data suggest that by helping identify which patients have sufficient ischemia to merit revascularization, stress perfusion imaging may play a significant role in the selection of patients for catheterization within a strategy based on the

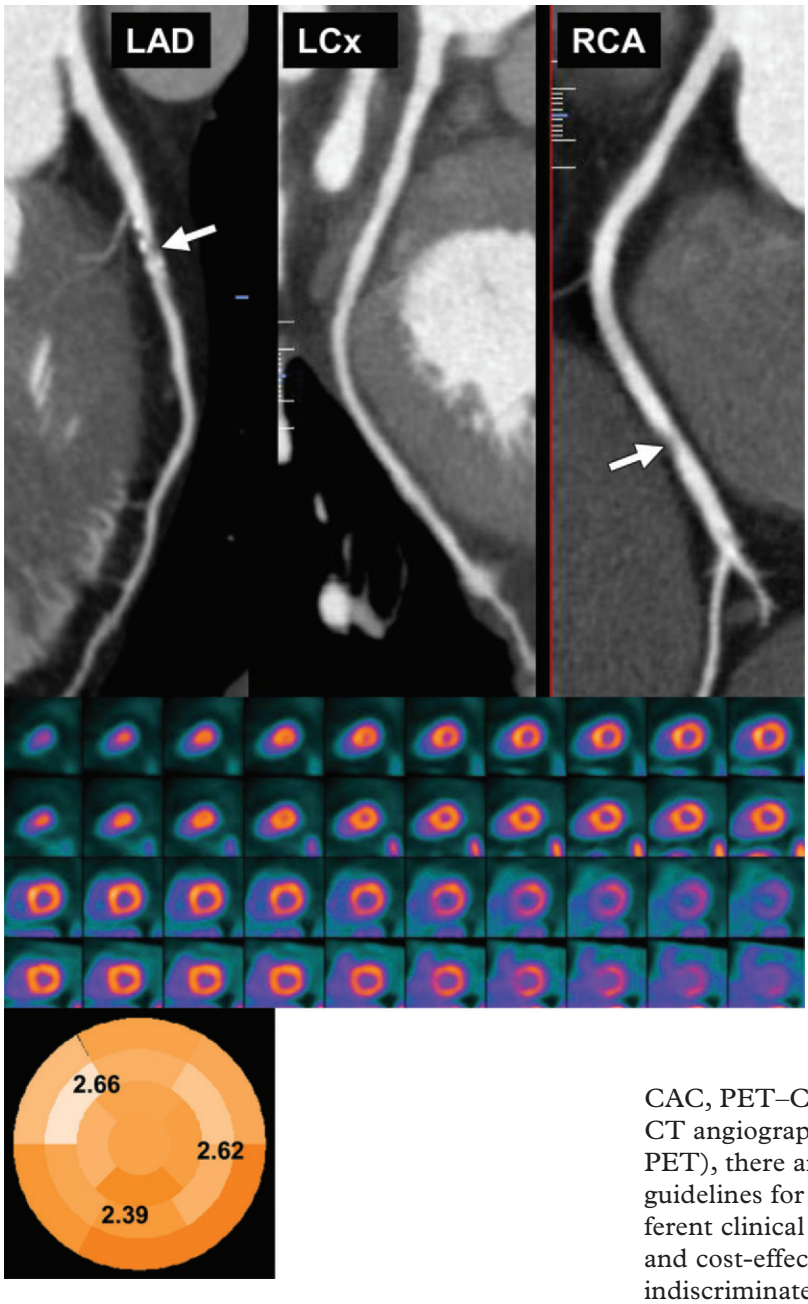

Figure 8. Potential added value of myocardial perfusion CT in a 62-year-old man with atypical chest pain. Curved multiplanar reformatted coronary CT angiographic images (top) demonstrate mixed plaques with moderately significant stenosis in the proximal left anterior descending *(LAD)* artery (70%) and right coronary artery *(RCA)* (50%–70%) (arrow). *LCx* = left circumflex artery. Stress-rest short-axis PET scans (middle) show normal regional myocardial perfusion, and a parametric polar map (bottom) shows normal CFR (>2) in all three coronary territories, reflecting no evidence of flow-limiting CAD.

characterization of potential benefit. From the foregoing discussion, it is evident that this physiologic description of ischemia may have greater clinical impact than visually defined coronary anatomy for revascularization decision making.

Customization of Protocols

Although there are a multitude of PET-centered imaging options available (ie, PET alone, PET/CAC, PET–CT angiography, PET followed by CT angiography, CT angiography followed by PET), there are presently no comprehensive guidelines for an ideal testing strategy in different clinical scenarios. Radiation exposure and cost-effectiveness considerations prohibit indiscriminate use of a strategy combining all three imaging modalities in all patients. Instead, protocols should be tailored to the individual patient, taking into consideration *(a)* the pretest probability of epicardial stenoses and microvascular dysfunction, *(b)* renal function, and *(c)* the impact that test results would have on "downstream" management.

Conclusions

Myocardial perfusion PET is emerging as a powerful tool for the evaluation of patients with known or suspected CAD. PET appears to be more accurate and efficient than SPECT in the evaluation of CAD and can be performed at a significantly lower radiation dose. Key strengths of this method include its capacity to quantify rest–peak stress left ventricular systolic function as well as CFR, which together confer an important advantage over other methods for the detection of multivessel CAD and, potentially, for risk stratification. The integration of PET and CT for assessing the anatomic extent and functional consequences of CAD offers great potential for both diagnosis and management. Further validation of the prognostic value and cost effectiveness of PET is warranted.

***Disclosures of Potential Conflicts of Interest.*—M.F.D.C.:** *Related financial activities:* grant from Toshiba. *Other financial activities:* none.

References

1. Schelbert HR. Evaluation of myocardial blood flow in cardiac disease. In: Skorton DJ, Schelbert HR, Wolf GL, Brundage BH, eds. Cardiac imaging: a companion to Braunwald's heart disease. Philadelphia, Pa: Saunders, 1991; 1093–1112.
2. Shelton ME, Green MA, Mathias CJ, Welch MJ, Bergmann SR. Kinetics of copper-PTSM in isolated hearts: a novel tracer for measuring blood flow with positron emission tomography. J Nucl Med 1989;30 (11):1843–1847.
3. Shelton ME, Green MA, Mathias CJ, Welch MJ, Bergmann SR. Assessment of regional myocardial and renal blood flow with copper-PTSM and positron emission tomography. Circulation 1990;82(3): 990–997.
4. Beanlands RS, Muzik O, Mintun M, et al. The kinetics of copper-62-PTSM in the normal human heart. J Nucl Med 1992;33(5):684–690.
5. Herrero P, Hartman JJ, Green MA, et al. Regional myocardial perfusion assessed with generator-produced copper-62-PTSM and PET. J Nucl Med 1996;37(8):1294–1300.
6. Herrero P, Markham J, Weinheimer CJ, et al. Quantification of regional myocardial perfusion with generator-produced 62Cu-PTSM and positron emission tomography. Circulation 1993;87(1):173–183.
7. Proportional Technologies, Inc. 62Cu-PTSM studies. Available at: http://www.proportionaltech.com/new_site/index.php?option=com_content&view=article&id=88&Itemid=86. Accessed March 10, 2011.
8. Sherif HM, Saraste A, Weidl E, et al. Evaluation of a novel (18)F-labeled positron-emission tomography perfusion tracer for the assessment of myocardial infarct size in rats. Circ Cardiovasc Imaging 2009;2 (2):77–84.
9. Yu M, Bozek J, Guaraldi M, Kagan M, Azure M, Robinson SP. Cardiac imaging and safety evaluation of BMS747158, a novel PET myocardial perfusion imaging agent, in chronic myocardial compromised rabbits. J Nucl Cardiol 2010;17(4):631–636.
10. Yu M, Guaraldi MT, Mistry M, et al. BMS-747158-02: a novel PET myocardial perfusion imaging agent. J Nucl Cardiol 2007;14(6):789–798.
11. Nekolla SG, Reder S, Saraste A, et al. Evaluation of the novel myocardial perfusion positron-emission tomography tracer 18F-BMS-747158-02: comparison to 13N-ammonia and validation with microspheres in a pig model. Circulation 2009;119(17): 2333–2342.
12. Lantheous Medical Imaging. Lantheus Medical Imaging receives special protocol assessment approval from FDA for phase 3 trial of flurpiridaz F-18 for the diagnosis of coronary artery disease. Available at: http://www.radiopharm.com/News-Press-2011-0311.html. Accessed March 13, 2011.
13. Humm JL, Rosenfeld A, Del Guerra A. From PET detectors to PET scanners. Eur J Nucl Med Mol Imaging 2003;30(11):1574–1597.
14. Cherry SR. The 2006 Henry N. Wagner Lecture: of mice and men (and positrons)—advances in PET imaging technology. J Nucl Med 2006;47(11): 1735–1745.
15. Einstein AJ, Johnson LL, Bokhari S, et al. Agreement of visual estimation of coronary artery calcium from low-dose CT attenuation correction scans in hybrid PET/CT and SPECT/CT with standard Agatston score. J Am Coll Cardiol 2010;56(23): 1914–1921.
16. Higuchi T, Nekolla SG, Jankaukas A, et al. Characterization of normal and infarcted rat myocardium using a combination of small-animal PET and clinical MRI. J Nucl Med 2007;48(2):288–294.
17. Chow BJ, Beanlands RS, Lee A, et al. Treadmill exercise produces larger perfusion defects than dipyridamole stress N-13 ammonia positron emission tomography. J Am Coll Cardiol 2006;47(2):411–416.
18. Stabin MG. Radiopharmaceuticals for nuclear cardiology: radiation dosimetry, uncertainties, and risk. J Nucl Med 2008;49(9):1555–1563.
19. Senthamizhchelvan S, Bravo PE, Esaias C, et al. Human biodistribution and radiation dosimetry of 82Rb. J Nucl Med 2010;51(10):1592–1599.
20. Stabin MG. Proposed revision to the radiation dosimetry of 82Rb. Health Phys 2010;99(6):811–813.
21. Holly TA, Abbott BG, Al-Mallah M, et al. Single photon-emission computed tomography. J Nucl Cardiol 2010;17(5):941–973.
22. Senthamizhchelvan S, Bravo PE, Lodge MA, Merrill J, Bengel FM, Sgouros G. Radiation dosimetry of 82Rb in humans under pharmacologic stress. J Nucl Med 2011;52(3):485–491.
23. Yoshinaga K, Chow BJ, Williams K, et al. What is the prognostic value of myocardial perfusion imaging using rubidium-82 positron emission tomography? J Am Coll Cardiol 2006;48(5):1029–1039.
24. Goetze S, Wahl RL. Prevalence of misregistration between SPECT and CT for attenuation-corrected myocardial perfusion SPECT. J Nucl Cardiol 2007; 14(2):200–206.
25. Gould KL, Pan T, Loghin C, Johnson NP, Guha A, Sdringola S. Frequent diagnostic errors in cardiac PET/CT due to misregistration of CT attenuation and emission PET images: a definitive analysis of causes, consequences, and corrections. J Nucl Med 2007;48(7):1112–1121.

26. McQuaid SJ, Hutton BF. Sources of attenuation-correction artefacts in cardiac PET/CT and SPECT/CT. Eur J Nucl Med Mol Imaging 2008;35(6):1117–1123.
27. Slomka PJ, Le Meunier L, Hayes SW, et al. Comparison of myocardial perfusion 82Rb PET performed with CT- and transmission CT-based attenuation correction. J Nucl Med 2008;49(12):1992–1998.
28. Sampson UK, Dorbala S, Limaye A, Kwong R, Di Carli MF. Diagnostic accuracy of rubidium-82 myocardial perfusion imaging with hybrid positron emission tomography/computed tomography in the detection of coronary artery disease. J Am Coll Cardiol 2007;49(10):1052–1058.
29. Bateman TM, Heller GV, McGhie AI, et al. Diagnostic accuracy of rest/stress ECG-gated Rb-82 myocardial perfusion PET: comparison with ECG-gated Tc-99m sestamibi SPECT. J Nucl Cardiol 2006;13(1):24–33.
30. Marwick TH, Nemec JJ, Stewart WJ, Salcedo EE. Diagnosis of coronary artery disease using exercise echocardiography and positron emission tomography: comparison and analysis of discrepant results. J Am Soc Echocardiogr 1992;5(3):231–238.
31. Grover-McKay M, Ratib O, Schwaiger M, et al. Detection of coronary artery disease with positron emission tomography and rubidium 82. Am Heart J 1992;123(3):646–652.
32. Stewart RE, Schwaiger M, Molina E, et al. Comparison of rubidium-82 positron emission tomography and thallium-201 SPECT imaging for detection of coronary artery disease. Am J Cardiol 1991;67(16):1303–1310.
33. Go RT, Marwick TH, MacIntyre WJ, et al. A prospective comparison of rubidium-82 PET and thallium-201 SPECT myocardial perfusion imaging utilizing a single dipyridamole stress in the diagnosis of coronary artery disease. J Nucl Med 1990;31(12):1899–1905.
34. Demer LL, Gould KL, Goldstein RA, et al. Assessment of coronary artery disease severity by positron emission tomography: comparison with quantitative arteriography in 193 patients. Circulation 1989;79(4):825–835.
35. Tamaki N, Yonekura Y, Senda M, et al. Value and limitation of stress thallium-201 single photon emission computed tomography: comparison with nitrogen-13 ammonia positron tomography. J Nucl Med 1988;29(7):1181–1188.
36. Gould KL, Goldstein RA, Mullani NA, et al. Noninvasive assessment of coronary stenoses by myocardial perfusion imaging during pharmacologic coronary vasodilation. VIII. Clinical feasibility of positron cardiac imaging without a cyclotron using generator-produced rubidium-82. J Am Coll Cardiol 1986;7(4):775–789.
37. Di Carli MF, Hachamovitch R. New technology for noninvasive imaging of coronary artery disease. Circulation 2007;115(11):1464–1480.
38. Dorbala S, Vangala D, Sampson U, Limaye A, Kwong R, Di Carli MF. Value of vasodilator left ventricular ejection fraction reserve in evaluating the magnitude of myocardium at risk and the extent of angiographic coronary artery disease: a 82Rb PET/CT study. J Nucl Med 2007;48(3):349–358.
39. Brown TL, Merrill J, Volokh L, Bengel FM. Determinants of the response of left ventricular ejection fraction to vasodilator stress in electrocardiographically gated (82)rubidium myocardial perfusion PET. Eur J Nucl Med Mol Imaging 2008;35(2):336–342.
40. Lertsburapa K, Ahlberg AW, Bateman TM, et al. Independent and incremental prognostic value of left ventricular ejection fraction determined by stress gated rubidium 82 PET imaging in patients with known or suspected coronary artery disease. J Nucl Cardiol 2008;15(6):745–753.
41. Dorbala S, Hachamovitch R, Curillova Z, et al. Incremental prognostic value of gated Rb-82 positron emission tomography myocardial perfusion imaging over clinical variables and rest LVEF. JACC Cardiovasc Imaging 2009;2(7):846–854.
42. Di Carli M, Czernin J, Hoh CK, et al. Relation among stenosis severity, myocardial blood flow, and flow reserve in patients with coronary artery disease. Circulation 1995;91(7):1944–1951.
43. Uren NG, Melin JA, De Bruyne B, Wijns W, Baudhuin T, Camici PG. Relation between myocardial blood flow and the severity of coronary-artery stenosis. N Engl J Med 1994;330(25):1782–1788.
44. Beanlands RS, Muzik O, Melon P, et al. Noninvasive quantification of regional myocardial flow reserve in patients with coronary atherosclerosis using nitrogen-13 ammonia positron emission tomography: determination of extent of altered vascular reactivity. J Am Coll Cardiol 1995;26(6):1465–1475.
45. El Fakhri G, Kardan A, Sitek A, et al. Reproducibility and accuracy of quantitative myocardial blood flow assessment with (82)Rb PET: comparison with (13)N-ammonia PET. J Nucl Med 2009;50(7):1062–1071.
46. El Fakhri G, Sitek A, Guérin B, Kijewski MF, Di Carli MF, Moore SC. Quantitative dynamic cardiac 82Rb PET using generalized factor and compartment analyses. J Nucl Med 2005;46(8):1264–1271.
47. Anagnostopoulos C, Almonacid A, El Fakhri G, et al. Quantitative relationship between coronary vasodilator reserve assessed by 82Rb PET imaging and coronary artery stenosis severity. Eur J Nucl Med Mol Imaging 2008;35(9):1593–1601.
48. Yoshinaga K, Katoh C, Noriyasu K, et al. Reduction of coronary flow reserve in areas with and without ischemia on stress perfusion imaging in patients with coronary artery disease: a study using oxygen 15-labeled water PET. J Nucl Cardiol 2003;10(3):275–283.
49. Parkash R, deKemp RA, Ruddy TD, et al. Potential utility of rubidium 82 PET quantification in patients with 3-vessel coronary artery disease. J Nucl Cardiol 2004;11(4):440–449.
50. Dorbala S, Hassan A, Heinonen T, Schelbert HR, Di Carli MF. RAMPART investigators: coronary vasodilator reserve and Framingham risk scores in subjects at risk for coronary artery disease. J Nucl Cardiol 2006;13(6):761–767.
51. Herzog BA, Husmann L, Valenta I, et al. Long-term prognostic value of 13N-ammonia myocardial perfusion positron emission tomography added value of coronary flow reserve. J Am Coll Cardiol 2009;54(2):150–156.

52. Berman DS, Wong ND, Gransar H, et al. Relationship between stress-induced myocardial ischemia and atherosclerosis measured by coronary calcium tomography. J Am Coll Cardiol 2004;44(4):923–930.
53. Schenker MP, Dorbala S, Hong EC, et al. Interrelation of coronary calcification, myocardial ischemia, and outcomes in patients with intermediate likelihood of coronary artery disease: a combined positron emission tomography/computed tomography study. Circulation 2008;117(13):1693–1700.
54. Chang SM, Nabi F, Xu J, et al. The coronary artery calcium score and stress myocardial perfusion imaging provide independent and complementary prediction of cardiac risk. J Am Coll Cardiol 2009;54(20):1872–1882.
55. Dayanikli F, Grambow D, Muzik O, Mosca L, Rubenfire M, Schwaiger M. Early detection of abnormal coronary flow reserve in asymptomatic men at high risk for coronary artery disease using positron emission tomography. Circulation 1994;90(2):808–817.
56. Di Carli MF, Janisse J, Grunberger G, Ager J. Role of chronic hyperglycemia in the pathogenesis of coronary microvascular dysfunction in diabetes. J Am Coll Cardiol 2003;41(8):1387–1393.
57. Schindler TH, Cardenas J, Prior JO, et al. Relationship between increasing body weight, insulin resistance, inflammation, adipocytokine leptin, and coronary circulatory function. J Am Coll Cardiol 2006;47(6):1188–1195.
58. Pitkänen OP, Raitakari OT, Niinikoski H, et al. Coronary flow reserve is impaired in young men with familial hypercholesterolemia. J Am Coll Cardiol 1996;28(7):1705–1711.
59. Yokoyama I, Murakami T, Ohtake T, et al. Reduced coronary flow reserve in familial hypercholesterolemia. J Nucl Med 1996;37(12):1937–1942.
60. Kajander S, Joutsiniemi E, Saraste M, et al. Cardiac positron emission tomography/computed tomography imaging accurately detects anatomically and functionally significant coronary artery disease. Circulation 2010;122(6):603–613.
61. Hacker M, Jakobs T, Matthiesen F, et al. Comparison of spiral multidetector CT angiography and myocardial perfusion imaging in the noninvasive detection of functionally relevant coronary artery lesions: first clinical experiences. J Nucl Med 2005;46(8):1294–1300.
62. Schuijf JD, Wijns W, Jukema JW, et al. Relationship between noninvasive coronary angiography with multi-slice computed tomography and myocardial perfusion imaging. J Am Coll Cardiol 2006;48(12):2508–2514.
63. Di Carli MF, Dorbala S, Curillova Z, et al. Relationship between CT coronary angiography and stress perfusion imaging in patients with suspected ischemic heart disease assessed by integrated PET-CT imaging. J Nucl Cardiol 2007;14(6):799–809.
64. Rispler S, Roguin A, Keidar Z, et al. Integrated SPECT/CT for the assessment of hemodynamically significant coronary artery lesions [abstr]. J Am Coll Cardiol 2006;47(suppl):115A.
65. Hacker M, Jakobs T, Hack N, et al. Sixty-four slice spiral CT angiography does not predict the functional relevance of coronary artery stenoses in patients with stable angina. Eur J Nucl Med Mol Imaging 2007;34(1):4-10.
66. Gould KL. Identifying and measuring severity of coronary artery stenosis: quantitative coronary arteriography and positron emission tomography. Circulation 1988;78(2):237–245.
67. Meijboom WB, Van Mieghem CA, van Pelt N, et al. Comprehensive assessment of coronary artery stenoses: computed tomography coronary angiography versus conventional coronary angiography and correlation with fractional flow reserve in patients with stable angina. J Am Coll Cardiol 2008;52(8):636–643.
68. Shaw LJ, Hachamovitch R, Berman DS, et al. The economic consequences of available diagnostic and prognostic strategies for the evaluation of stable angina patients: an observational assessment of the value of precatheterization ischemia. Economics of Noninvasive Diagnosis (END) Multicenter Study Group. J Am Coll Cardiol 1999;33(3):661–669.
69. Weiner DA, Ryan TJ, McCabe CH, et al. The role of exercise testing in identifying patients with improved survival after coronary artery bypass surgery. J Am Coll Cardiol 1986;8(4):741–748.
70. Hachamovitch R, Hayes SW, Friedman JD, Cohen I, Berman DS. Comparison of the short-term survival benefit associated with revascularization compared with medical therapy in patients with no prior coronary artery disease undergoing stress myocardial perfusion single photon emission computed tomography. Circulation 2003;107(23):2900–2907.
71. Shaw LJ, Berman DS, Maron DJ, et al. Optimal medical therapy with or without percutaneous coronary intervention to reduce ischemic burden: results from the Clinical Outcomes Utilizing Revascularization and Aggressive Drug Evaluation (COURAGE) trial nuclear substudy. Circulation 2008;117(10):1283–1291.
72. Tonino PA, De Bruyne B, Pijls NH, et al. Fractional flow reserve versus angiography for guiding percutaneous coronary intervention. N Engl J Med 2009;360(3):213–224.

Cardiac PET/CT for the Evaluation of Known or Suspected Coronary Artery Disease[1]

Marcelo F. Di Carli, MD • Venkatesh L. Murthy, MD, PhD

RadioGraphics 2011; 31:1239–1254 • **Published online** 10.1148/rg.315115056 • **Content Codes:** CA CT NM

Page 1243
PET with the use of short-lived radiopharmaceuticals results in substantially lower radiation doses to patients than does SPECT (18).

Page 1243
Although severe artifacts resulting in suboptimal imaging are far less common with PET than with SPECT (23), artifacts due to errors in attenuation correction are common and have been reported with PET/CT in 30%–60% of cases (24,25).

Page 1245 (Figure on page 1245)
Although the assessment of myocardial perfusion with PET remains a sensitive means of diagnosing or ruling out the presence of obstructive CAD in individual patients, PET (like SPECT) often helps identify only the coronary territory affected by the most severe stenoses. This is because coronary vasodilator reserve is globally reduced in patients with diffuse CAD, leading to so-called balanced reduction in myocardial perfusion and limiting detection of multivessel coronary artery stenosis (Fig 3).

Page 1247
These data also confirmed that LVEF and stress perfusion imaging yield independent and additive prognostic information.

Page 1248
The difficulties in identifying balanced flow reduction in high-risk patient groups (eg, patients with diabetes mellitus or renal dysfunction) can be overcome with quantitative myocardial perfusion measures. Thus, better delineation of at-risk myocardium with quantitative CFR may also improve risk stratification in patients with known or suspected CAD.